JOURNAL OF THE KOREAN ASTRONOMICAL SOCIETY
36: 111 ~ 121, 2003

COSMIC RAY ACCELERATION AT COSMOLOGICAL SHOCKS: NUMERICAL SIMULATIONS OF CR MODIFIED PLANE-PARALLEL SHOCKS

HYESUNG KANG
Department of Earth Sciences, Pusan National University, Pusan 609-735, Korea
E-mail: kang@uju.es.pusan.ac.kr
(Received November 16, 2002; Accepted August 17, 2003)

ABSTRACT

In order to explore the cosmic ray acceleration at the cosmological shocks, we have performed numerical simulations of one-dimensional, plane-parallel, cosmic ray (CR) modified shocks with the newly developed CRASH (Cosmic Ray Amr SHock) numerical code. Based on the hypothesis that strong Alfvén waves are self-generated by streaming CRs, the Bohm diffusion model for CRs is adopted. The code includes a plasma-physics-based "injection" model that transfers a small proportion of the thermal proton flux through the shock into low energy CRs for acceleration there. We found that, for strong accretion shocks with Mach numbers greater than 10, CRs can absorb most of shock kinetic energy and the accretion shock speed is reduced up to 20 %, compared to pure gas dynamic shocks. Although the amount of kinetic energy passed through accretion shocks is small, since they propagate into the low density intergalactic medium, they might possibly provide acceleration sites for ultra-high energy cosmic rays of $E > 10^{18}$eV. For internal/merger shocks with Mach numbers less than 3, however, the energy transfer to CRs is only about 10-20 % and so nonlinear feedback due to the CR pressure is insignificant. Considering that intracluster medium (ICM) can be shocked repeatedly, however, the CRs generated by these weak shocks could be sufficient to explain the observed non-thermal signatures from clusters of galaxies.

Key words : acceleration of particles – cosmology – cosmic rays – hydrodynamics – methods: numerical

I. INTRODUCTION

During the structure formation in the universe large-scale collisionless shocks are produced by flow motions associated with the gravitational collapse of nonlinear structures. Estimated speed and curvature radius of these shocks could be as large as a few 1000 km/s and several Mpc, respectively. These shocks not only heat the intergalactic medium (IGM) to a few to 10 KeV, but also can accelerate the cosmic-ray (CR) ions and electrons to very high energies (Norman, Melrose & Achterberg 1995; Kang, Ryu & Jones 1996; Kang, Rachen & Biermann 1997).

In this contribution we will first review our current understandings on theoretical and observational aspects of cosmological shocks and particle acceleration. We then present numerical simulation results for quasi-parallel shocks in 1D plane-parallel geometry with the physical parameters relevant for the cosmological shocks emerging in large scale structure formation of the Universe.

(a) Properties of Cosmological Shocks

In general, cosmic shocks associated with large scale structure formation can be oblique and complex in morphology, depending on the types of nonlinear structure onto which the accretion flow falls. They can be classified into three types: 1D plane-parallel shocks around the sheets, 2D cylindrical shocks around the filaments, and 3D spherical shocks around the clusters of galaxies. A simple analytic treatment, however, can be sufficient to elucidate the general properties of cosmological shocks. According to self-similar solutions of 1D spherical accretion in the Einstein-de Sitter universe (Bertschinger 1985, Ryu & Kang 1997, Miniati *et al.* 2000), the characteristics of accretion shocks are given as

$$R_s = 2.12 h^{-1}\mathrm{Mpc}\left(\frac{M_{cl}}{10^{15}h^{-1}\mathrm{M}_\odot}\right)^{1/3}, \quad (1)$$

$$T_{cl}(0.3R_s) = 6.06\ \mathrm{keV}\left(\frac{M_{cl}}{10^{15}h^{-1}\mathrm{M}_\odot}\right)^{2/3}, \quad (2)$$

$$V_s = 1.31\times 10^3 \mathrm{km\ s^{-1}}\left(\frac{M_{cl}}{10^{15}h^{-1}\mathrm{M}_\odot}\right)^{1/3}. \quad (3)$$

Here R_s is the shock radius, T_{cl} is the temperature at $r = 0.3R_s$, V_s is the accretion shock speed, and M_{cl} is the total cluster mass.

With the Bohm diffusion model for Fermi first-order acceleration, the maximum proton momentum acceler-

Proceedings of the APCTP Workshop on *Formation and Interaction of Galaxies*

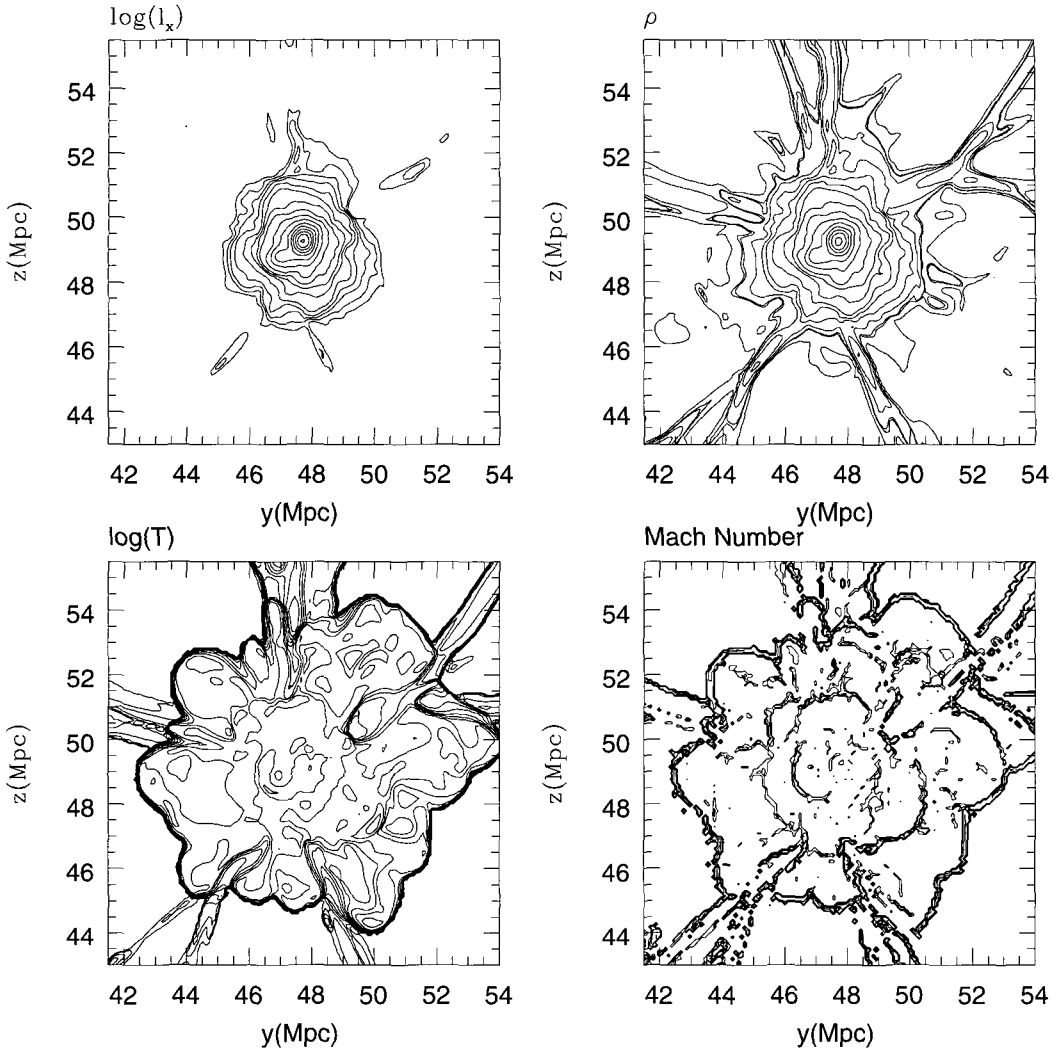

Fig. 1.— 2D slice of $(12.5\ h^{-1}\ \mathrm{Mpc})^2$ from a LCDM simulation. X-ray emissivity, gas density, temperature, and Mach number of shocks are shown. The central cluster is in a filament which lies along the direction perpendicular to the y-z plane. Thin features around the cluster are pancakes intersecting at the location of the cluster.

ated by a cosmological shock can be calculated by

$$(\frac{p_{\rm max}}{10^{10}}) \approx (\frac{\tau_{age}}{8\times 10^9 {\rm yrs}}) B_\mu (\frac{V_s}{1000 {\rm km\ s^{-1}}})^2, \quad (4)$$

where τ_{age} is the age of the shock and B_μ is the magnetic field strength in units of microgauss. Here we use the jump conditions in strong shock limit and assume for a turbulent field that B/ρ is constant across the shock. This shows that the cluster accretion shocks can accelerate the CR protons up to 10^{19}eV in a cosmological time scale. The diffusion length of the CR protons is given by

$$D_{\rm diff} = 1.02{\rm Mpc}(\frac{p}{10^{10}}) B_\mu^{-1} (\frac{V_s}{1000 {\rm km\ s^{-1}}})^{-1}. \quad (5)$$

So the CR protons of $E = 10^{19}$eV diffuse on the length scale comparable to the cluster size and can be confined by the cluster accretion shocks.

Figure 1 shows the X-ray emissivity, gas density, temperature, and Mach number of cosmological shocks in a two-dimensional slice of a simulated LCDM universe (Kang, Ryu, & Song 2002) centered around a rich cluster. Thin features protruding around the cluster are in fact cross sections of several intersecting pancakes. The temperature and Mach number contour maps show that the radius of strong accretion shocks for this particular cluster is about $5h^{-1}$Mpc, and that there are many more weaker internal shocks around the cluster within $5h^{-1}$Mpc region. Some of those weak shocks can be considered as "merger shocks" that are formed by merging substructures. Detailed flow velocity field around this cluster is shown in Figure 2,

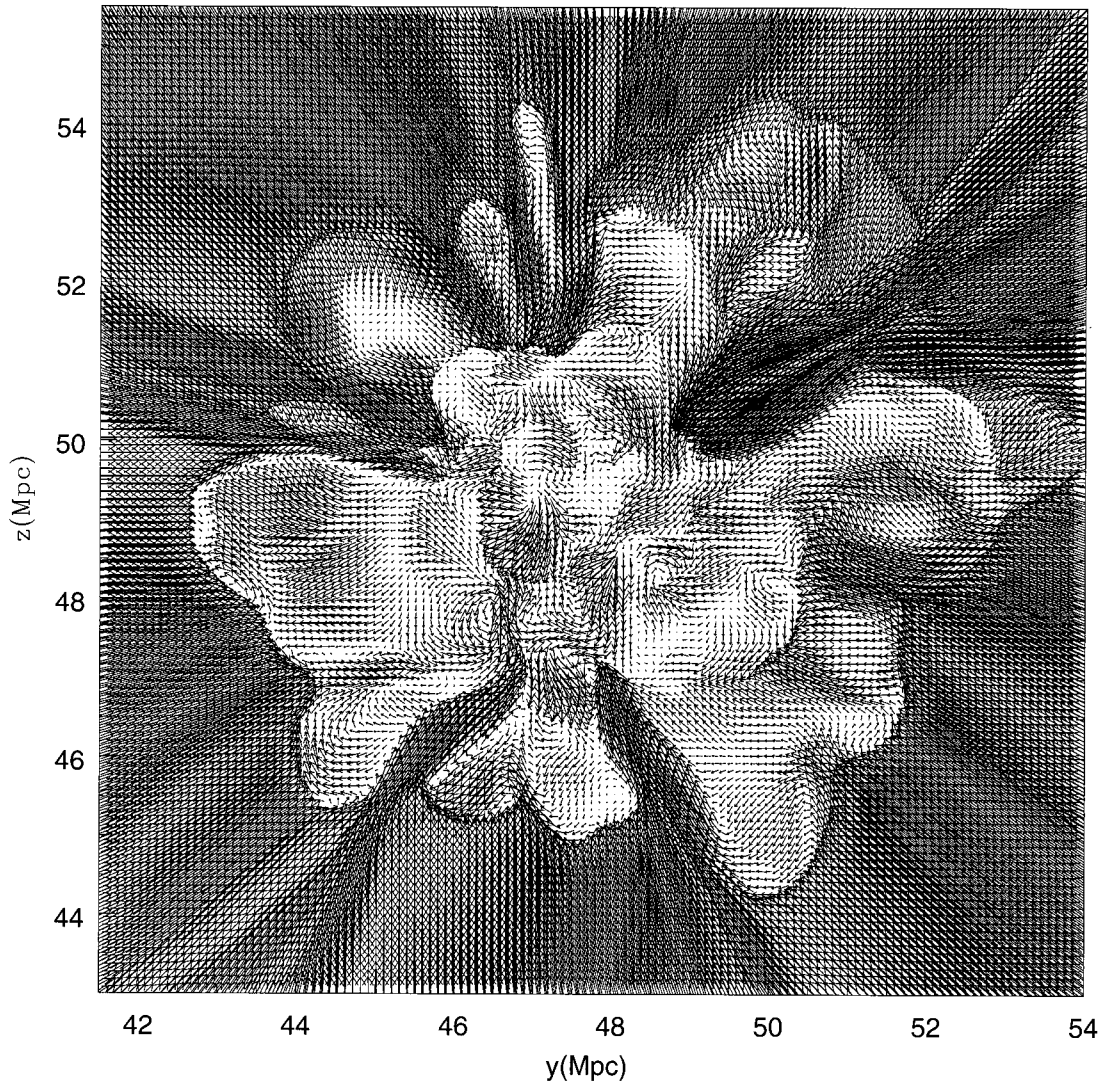

Fig. 2.— 2D flow velocity field in the plane shown in Figure 1.

which also shows rich and complex internal flow motions, reflecting the hierarchical clustering process on relevant scales. This demonstrates that shocks are abundant in the IGM around clusters and inside filaments, and the pancakes are bounded by accretion shocks. We calculated the time-integrated amount of kinetic energy passed through shock surfaces from z=2 to z=0 by $E_{kin}(M) = \int dt \int (dl)^2 0.5 \rho_1 V_s^3$ as a function of shock Mach number. The fraction of the shock kinetic energy that would be transferred to CRs is estimated from the CR shock simulations of Kang, Jones & Gieseler (2002), while the fraction that is converted to the gas thermal energy is calculated from the shock jump condition. We found about 20 % of the shock kinetic energy is converted to the gas thermal energy, while about 10 % is transfered to the CR energy. The distributions of the kinetic, thermal, and CR energies as a function of shock mach number, that is, $E_{kin}(M), E_{th}(M), E_{cr}(M)$, show that most of thermal and CR energies are generated by internal weak shocks of $M < 5$ and the shocks with $M \sim 3$ contribute the most to CR energy generation (Ryu *et al.* 2002). This is because these internal weak shocks pass through the high density medium, while strong accretion shocks propagate into the low density medium.

(b) Observed Nonthermal Activities in Clusters

Recently there have been increasingly more observational evidences indicating signatures of nonthermal activities in galaxy clusters. There are now more than 25 clusters with diffuse radio emission that originates from CR electrons gyrating around the magnetic field in the intracluster medium (ICM) (Giovannini & Fer-

etti 2000). Depending on its observed properties the diffuse radio emission is further classified as either a *radio halo* when its morphology is regular and typically centered on and resembling the X-ray emissivity, or as a *radio relic* when it is irregular and located at the periphery of the cluster. Radio halos are usually found in rich clusters with high ICM temperature and high X-ray luminosity. The clusters with a radio halo and/or a relic show some signatures of recent merger events and significant substructures, but no cooling flows. The strong correlation between the radio power emitted at 1.4 GHz and the cluster X-ray luminosity, and the similarity of X-ray and radio morphology of radio halo clusters indicate a possible connection between the nonthermal and thermal energy components.

In addition to diffuse radio emission, recent observations in EUV and hard X-ray have also revealed that some clusters possess excess radiation compared to what is expected from the hot, thermal X-ray emitting ICM (*e.g.,* Sarazin & Lieu 1998; Lieu *et al.* 1999; Ensslin *et al.* 1999; Fusco-Femiano *et al.* 1999; Sarazin 1999). One mechanism proposed for the origin of this component is the inverse Compton (IC) scattering of cosmic microwave background photons by CR electrons accelerated by merger shocks and accretion shocks around the clusters. Also it has been suggested that significant fraction of the diffuse gamma-ray background radiation could originate from the same process (Loeb & Waxman 2000, Miniati 2002, Scharf & Mukherjee 2002). The same mechanisms that are capable of producing these CR electrons may have produced CR protons, although the existence of CR protons in the ICM has not yet been directly observed. The existing evidence for substantial CR populations in these environments argues that nonthermal activities in the ICM could be important in understanding the dynamical status and the evolution of the ICM (Sarazin & Lieu 1998; Lieu *et al.* 1999). CR protons and electrons may provide a significant pressure to the ICM, perhaps, comparable to the thermal gas pressure (Lieu *et al.* 1999, Colafrancesco 1999), as it is for the galactic CRs in the ISM of our own Galaxy. Collisions of CR protons in the ICM generate a flux of γ-ray photons through the production and subsequent decay of neutral pions. While such γ-rays have not yet been detected from clusters recent estimates have shown that γ-ray fluxes from the nearest rich clusters, such as Coma, are within the range of what may be detected by the next generation of γ-ray observatories (Ensslin *et al.* 1997, Sreekumar *et al.* 1996, Miniati *et al.* 2001)

(c) Magnetic Fields in IGM

Most astrophysical shocks are so-called "collisionless shocks" which form in a tenuous plasma via electromagnetic "viscosities," *i.e.,* collective electromagnetic interactions between the particles and the underlying irregular magnetic fields. Hence the existence of magnetic field in the IGM, especially its irregular component, is prerequisite to the shock formation process and heating of the ICM by cosmological shocks. The magnetic field in the interstellar medium of our Galaxy is about 5-8 μG. In fact a magnetic field with a typical strength of a few microgauss and a principal length scale of 10-100 kpc are commonly detected in most clusters of galaxies (*e.g.,* Kim, Kronberg, Tribble 1991, Kronberg 1994, Taylor *et al.* 1994, Feretti *et al.* 1995, Clarke *et al.* 2001, Carilli & Taylor 2002). Magnetic fields in the ICM can be measured using a variety of techniques: for example, 1) studies of synchrotron relic and halo radio sources within clusters indicates 0.4-1 μG. 2) studies of inverse Compton X-ray emission indicates 0.2-1 μG. 3) surveys of Faraday rotation measures of radio sources both within and behind clusters indicates 1-40 μG (Carilli & Taylor 2002). Magnetic fields may have been injected into the ICM by radio galaxies. They may have been seeded at shocks in the course of structure formation, and then stretched and amplified up to 0.1-1 microgauss levels by turbulent flow motions in ICM and also in filaments and sheets (Kulsrud *et al.* 1997, Ryu, Kang & Biermann 1998).

Observations of radio synchrotron emission and IC scattering of CMBR by CR electrons can provide a way to estimate the energy densities of CR electrons and magnetic fields in the ICM. For example, the CR electrons dominate over the magnetic field in terms of energy density, $E_{\rm CR\ electrons} \sim 100 E_{\rm magnetic\ fields}$, in Coma cluster (Fusco-Femiano *et al.* 1999). If we assume that the same mechanisms accelerating CR electrons also produce CR protons, they could provide a substantial fraction of the total pressure in the ICM (Sarazin & Lieu 1998). Thus it would be possible that $E_{\rm gas} \gtrsim E_{\rm CR\ protons} \gtrsim E_{\rm magnetic\ fields} \sim (10-100) E_{\rm CR\ electrons}$ in the ICM.

(d) Diffusive Shock Acceleration

It is now widely believed that CRs are diffusively accelerated at astrophysical shocks by the first-order Fermi process (Drury 1983; Blandford & Eichler 1987). For parallel shocks, in which the ambient magnetic field is aligned with the shock normal, the applicability of diffusive shock acceleration (DSA) theory is now fairly well established. Also it has been quite successful in explaining many aspects of the cosmic ray (CR) population, such as the nearly power-law spectrum of the CRs detected at the top of the atmosphere, the relation between the break in the power-law around the $\sim 10^{14}$ eV knee energy to the maximum energy of the CRs achievable in supernova remnants (SNRs), and, also the non-thermal, power-law electron populations deduced from the radio synchrotron observations of SNRs. According to the theory a significant fraction (up to 90%) of the kinetic energy of the bulk flow associated with the strong shock can be converted into CR protons, depending the CR injection rate (Jones & Kang 1990, Berezhko, Ksenofontov, & Yelshi 1995). If as much as

$10^{-4} - 10^{-3}$ of the particle flux passing through the shock were injected into the CR population, the CR pressure would dominate and the nonlinear feedback to the underlying flow would become substantial.

Plasma simulations of quasi-parallel shocks (Quest 1988) have shown that the particle velocity distribution has some residual anisotropy in the local fluid frame due to the incomplete isotropization during the collisionless shock formation process and so some particles can stream back upstream of the shock. Streaming motions of high energy particles against the background fluid generate strong MHD Alfvén waves upstream of the shock, which in turn scatter particles and prevent them from escaping upstream (e.g., Wentzel 1974; Bell 1978; Quest 1988;Lucek & Bell 2000). Due to these self-generated MHD waves thermal particles are confined and advected downstream, while some suprathermal particles in the high energy tail of the Maxwellian velocity distribution may re-cross the shock upstream. Then these particles are scattered back downstream by those same waves and can be accelerated further to higher energies via Fermi first order process. Hence the non-thermal, cosmic-ray particles are natural byproducts of the collisionless shock formation process and they are extracted from the shock-heated thermal particle distribution (Malkov & Völk 1998, Malkov & Drury 2001).

Gieseler, Jones & Kang (2000) have developed a numerical scheme that self-consistently incorporates this "thermal leakage injection" based on the analytic, nonlinear calculations of Malkov (1998). This injection scheme then has been implemented into the combined gas dynamics and the CR diffusion-convection code with the Adaptive Mesh Refinement technique by Kang, Jones & Giesler (2002). The resulting code was named as CRASH (Comic-Ray Amr SHock) code. The CR injection and acceleration efficiencies at quasi-parallel, plane-parallel shocks were calculated for a wide range of Mach numbers. They found that about 10^{-3} of incoming thermal particles are injected into the CRs, that up to 60 % of initial shock kinetic energy is transferred to CRs for strong shocks, and that the shock speed is reduced up to $\sim$ 17 % for shocks with Mach number greater 30.

Recently Kang & Jones (2002) have considered the CR acceleration at cosmological shocks, which are likely to emerge during the structure formation, by numerical simulations of plane-parallel CR shocks using the CRASH code. They found that for strong accretion shocks of $M_s > 10$, CRs can absorb most of shock kinetic energy and the accretion shock speed can be reduced up to 20 %, compared to pure gas dynamic shocks. For internal merger shocks of $M_s < 3$ the energy transfer to CRs should be less than 10-20 % of the shock kinetic energy at each shock passage, with an associated CR particle fraction of 10^{-3}. In this contribution we suggest that CR acceleration at cosmological shocks can have significant impacts on the structure formation, and that the ICM and the intergalactic space in filaments and pancakes are filled with the CR ions and electrons accelerated by those shocks.

In the next section we briefly describe the CRASH code. Then we review the numerical simulations of 1D parallel CR modified shocks and the main results in sections III and IV. Finally conclusions are given in §V.

II. CRASH CODE

(a) AMR Method with a Shock Tracking

With our CRASH code we solve the CR diffusion-convection equation for the CR distribution function, $f(p, x, t)$, along with CR modified gasdynamic equations. In order to overcome the problem of large dynamic range of diffusion length scales when a realistic diffusion transport model with a steeply momentum-dependent diffusion coefficient is adopted, we have combined an "Adaptive Mesh Refinement" (AMR) technique (Berger & Le Veque 1998) and a "shock tracking" technique (Le Veque & Shyue 1995), and implemented them into a hydro/CR code based on the wave-propagation method (Kang *et al.* 2001; Kang *et al.* 2002). The AMR technique allows us to "zoom in" inside the precursor structure with a hierarchy of small, refined grid levels applied around the shock. The shock tracking technique follows hydrodynamical shocks within regular zones and maintains them as true discontinuities, thus allowing us to refine the region around the gas subshock at an arbitrarily fine level. The readers are referred to Kang et al. (2002) for the further details.

(b) Injection Model

In the "thermal leakage" injection model, some suprathermal particles in the tail of the Maxwellian distribution swim successfully against the Alfvén waves advecting downstream, and then leak upstream across the subshock and get injected in the CR population. In order to model this injection process we adopted a "transparency function", $\tau_{\rm esc}(v, \epsilon)$, which expresses the probability that supra-thermal particles at a given velocity (v) can leak upstream through the magnetic waves, based on non-linear particle interactions with self-generated waves (Malkov and Völk 1998). The only free parameter of the adopted transparency function is the inverse wave-amplitude parameter, $\epsilon = B_0/B_\perp$, which measures the ratio of the amplitude of the post-shock MHD wave turbulence $B_\perp$ to the general magnetic field aligned with the shock normal, B_0. Fortunately, it is rather well constrained, since $0.3 \lesssim \epsilon \lesssim 0.4$ is indicated for strong shocks (Malkov & Völk 1998). The breadth of the thermal velocity distribution relative the downstream flow velocity in the subshock rest-frame (*i.e.*, $v_{\rm th}/u_d$) determines the probability of leakage, and so the injection process is sensitive to the velocity jump at the subshock, which depends on the subshock Mach number, $M_{\rm sub}$. We found that the injection rate increases with the subshock Mach number,

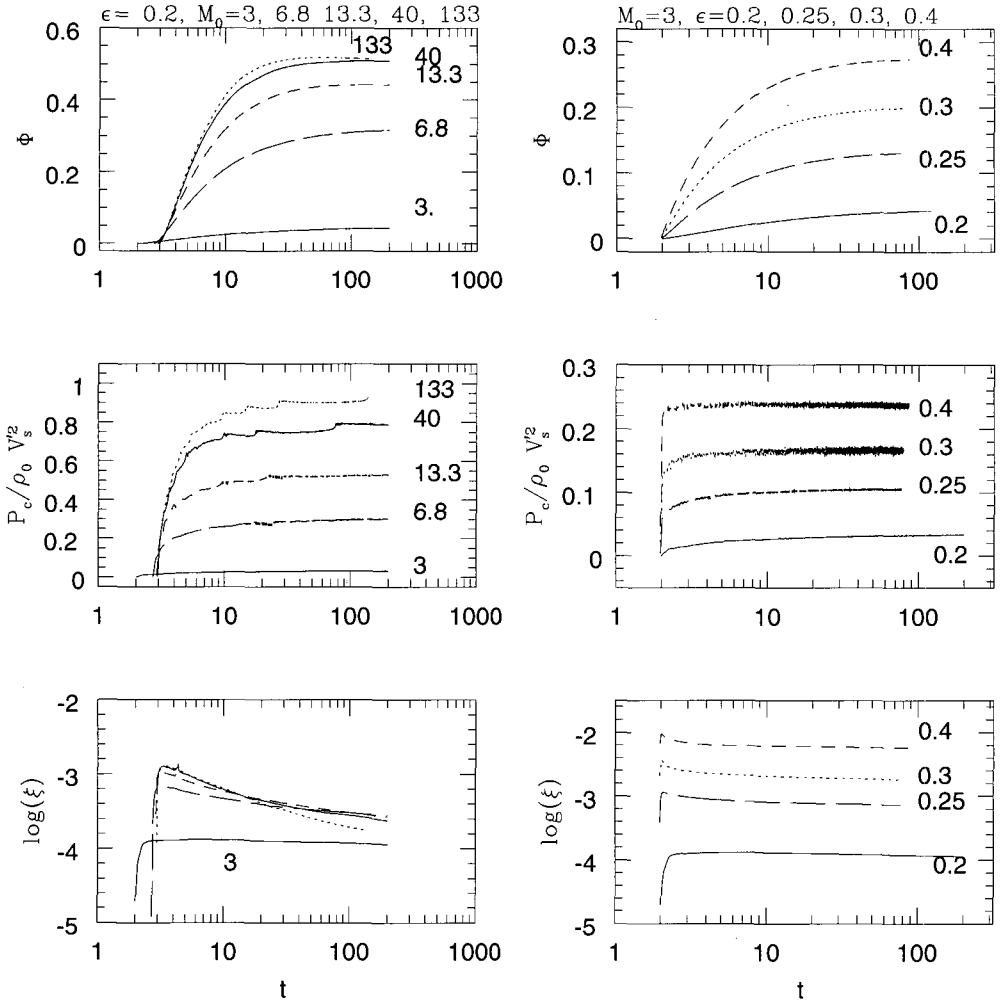

Fig. 3.— Time evolution of the shock driven by an accretion flow with $\rho_0 = 1$ and $u_0 = -1$ which is reflected at $x = 0$. The Mach number of the shock is $M_s = 13.3$. Seven levels of refinements ($l_{\max} = 7$) were used and the inverse wave-amplitude parameter $\epsilon = 0.2$ was adopted. The snapshots are shown at $t = 5$, 10, 50, 150, and 200. The right-facing shock propagates to the right, so the leftmost profile corresponds to the earliest time. For $t = 200$, data at each cell is shown as filled circles to show clearly the subshock jump. Note the distance from the reflecting plane is in a logarithmic scale.

but becomes independent of $M_{\rm sub}$ in the strong shock limit of $M_{\rm sub} \gtrsim 10$ (Kang *et al.* 2002).

In the CRASH code, in order to emulate numerically thermal leakage injection, we first estimate the number of suprathermal particles that cross the shock according to the diffusion-convection equation, and then we allow only a small fraction of the combined advective and diffusive fluxes to leak upstream with the probability prescribed by $\tau_{\rm esc}$. The readers are referred to Gieseler *et al.* (2001) for more details of our numerical scheme for thermal leakage injection model.

Although the theoretically preferred values of the inverse wave-amplitude parameter, ϵ, lie between 0.3 and 0.4 for strong shocks, such values lead to very efficient initial injection and most of the shock energy is transfered to the CR component for strong shocks of $M_s \gtrsim 30$ (Kang *et al.* 2002). As a more conservative option we have considered a set of models for $3 \le M_s \le 133$ with $\epsilon = 0.2$ and another set of models for $M_s = 3$ with $0.2 \le \epsilon \le 0.4$. The former is chosen to explore the dependence of the CR acceleration on the accretion flow Mach number for a given value of ϵ, while the latter is chosen to explore the dependence on the value of ϵ for a low Mach number shock. It is expected that the wave generation is weaker for low Mach shocks, leading to larger values of ϵ.

(c) Particle Diffusion Model

The Bohm diffusion model represents a saturated wave spectrum and gives the minimum diffusion coefficient as $\kappa_{\rm B} = 1/3 r_{\rm g} v$, when the particles scatter within one gyration radius ($r_{\rm g}$) due to random scatterings off

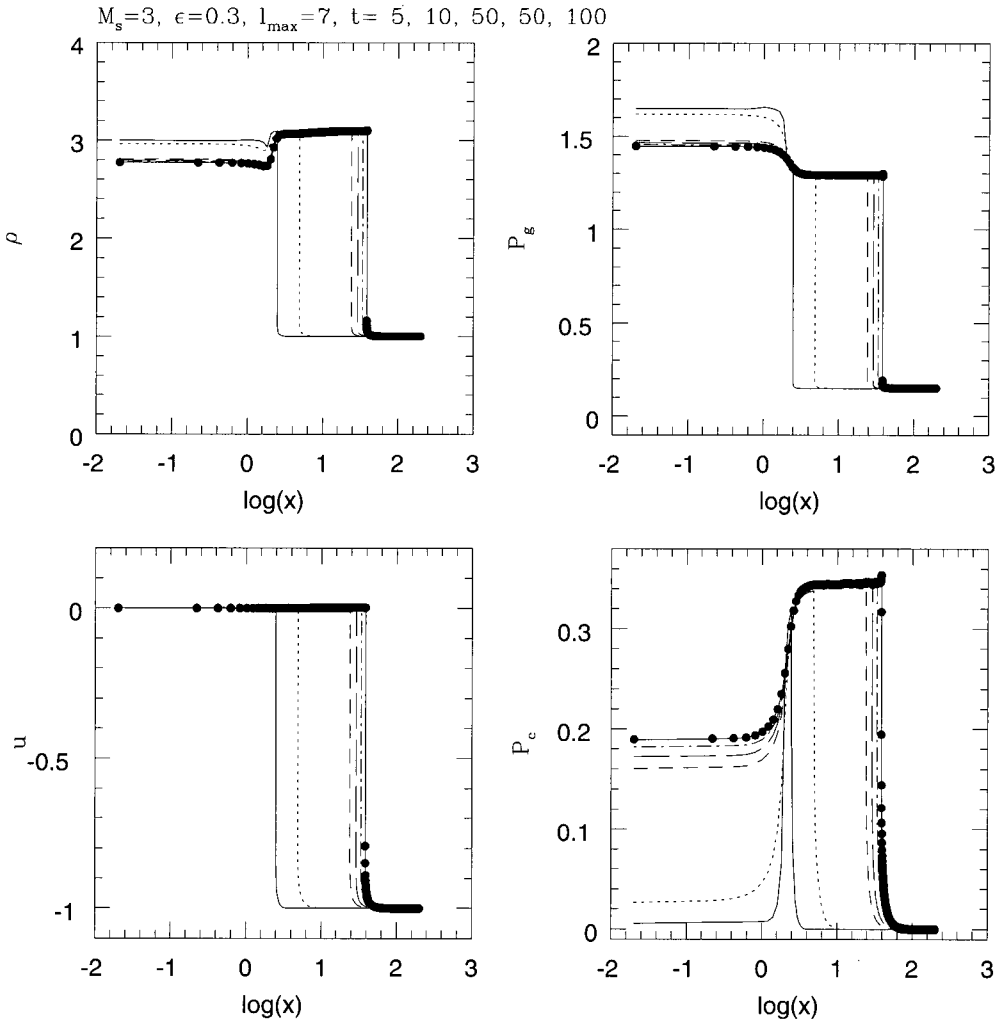

Fig. 4.— Same as Figure 3 except the shock Mach number is $M_s = 3$ and $\epsilon = 0.3$. The snapshots are shown at $t = 5$, 10, 50, and 100. For $t = 100$, data at each cell is shown as filled circles to show clearly the subshock jump.

the self-generated waves. This gives

$$\kappa(p) = \kappa_0 \frac{p^2}{(p^2+1)^{1/2}}, \qquad (6)$$

where $\kappa_0 = 3.13 \times 10^{22} \mathrm{cm^2 s^{-1}} B_\mu^{-1}$ and B_μ is the magnetic field strength in units of microgauss.

III. PANCAKE SHOCK MODELS

In Kang & Jones (2002) we have calculated CR acceleration at 1D cosmological pancake shocks formed by the steady accretion flow with a constant density and pressure. An accretion flow enters into the right boundary of the simulation box with a constant density, ρ_0, pressure, $P_{g,0}$, and velocity, u_0. The flow is reflected at the left boundary (*i.e.*, pancake middle plane) and a shock forms and propagates to the right. For convenience, we considered the accretion velocity of $u_0 = -1500 \mathrm{kms}^{-1}$ and the magnetic field of 1 microgauss as fiducial values for our simulations. For a hydrodynamic shock with no CRs, the shock speed is $V_s = |u_0| r/(r-1)$ in the rest frame of far upstream flow, where r is the compression ratio across the shock. We denote the shock strength with the shock Mach number $M_s = V_s/c_{s,0}$ where $c_{s,0}$ is the sound speed of the far upstream gas. Due to severe requirements on the computational resources, our simulations can follow the acceleration of the protons from suprathermal energies ($p \sim 10^{-3}$) to mildly relativistic energies ($p \sim 50$). For the particles in this energy range, the acceleration time scales are much shorter than and the cosmological time scale and the diffusion length scales are much smaller than the curvature of multi-dimensional cosmic shocks. On those scales where $D_{\mathrm{diff}} \ll R_s$, the diffusion and acceleration of CRs can be studied with the 1D plane-parallel shock models.

Figures 3 and 4 show the time evolution of shocks

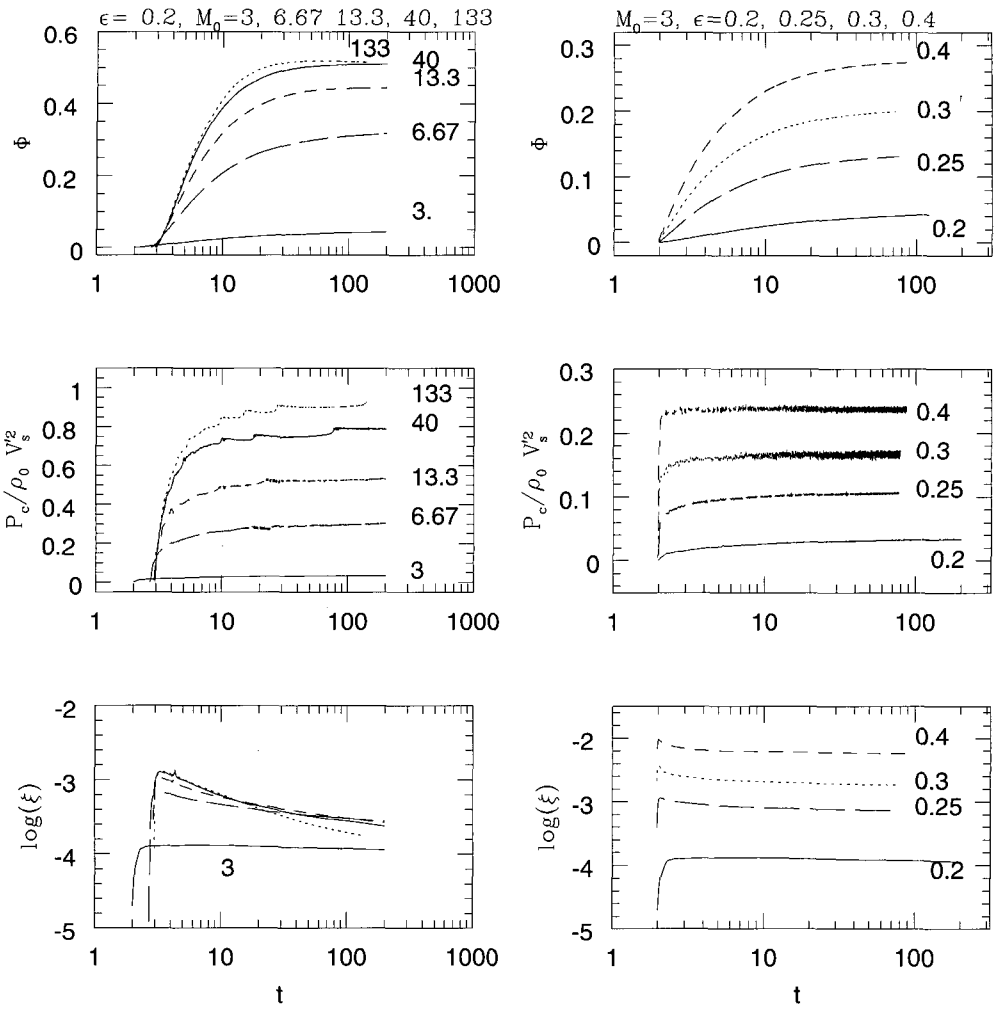

Fig. 5.— The ratio of total CR energy in the simulation box to the kinetic energy in the initial shock rest frame that has entered the simulation box from upstream, $\Phi(t)$, the postshock CR pressure in units of far upstream ram pressure in the instantaneous shock frame, and time-averaged injection efficiency, $\xi(t)$. Left three panels are for $M_s = 3 - 133$ and $\epsilon = 0.2$. Right three panels show the same quantities for $M_s = 3$ and $\epsilon = 0.2$, 0.25, 0.3, and 0.4.

for models with the shock Mach number, $M_s = 13.3$ and $M_s = 3$, respectively. The inverse wave amplitude parameter was assumed to be $\epsilon = 0.2$ for $M_s = 13.3$ and $\epsilon = 0.3$ for $M_s = 3$, considering the fact that the self-generated waves are weaker and so the leakage is likely more efficient at weaker shocks. In these figures the length and time scale are expressed in units of the diffusion length, $x_o = \kappa_o/|u_o|$, and the diffusion time, $t_o = \kappa_o/u_o^2$, respectively. The gas density and pressure normalization constants, ρ_o and $P_o = \rho_o u_o^2$, are arbitrary. For the shock of $M_s = 13.3$, as CRs are injected and accelerated, the CR pressure increases and diffuses upstream, leading to a precursor in which the upstream flow is decelerated and compressed adiabatically. As the CR precursor grows, the subshock slows down and the postshock density increases, while the postshock gas pressure decreases. The *instantaneous* shock speed relative to the far upstream flow, V_s', decrease up to 20 % from the initial shock speed, V_s. Because the injection rate is quite high for strong shocks, the CR energy increases and the modification to the flow structure proceeds very quickly in a time scale comparable to the acceleration time scale for $p \sim 2 - 3$. For the shock of $M_s = 3$, on the other hand, the growth of the precursor is minimal and the dynamical feed of CR pressure on the shock flow is not significant.

We observe the following general characteristics of the CR modified shocks:

- The total transition consists of a precursor and a subshock that weakens to a lower Mach number shock, but does not disappear entirely.
- After an initial quick adjustment, the CR pressure at the shock reaches *approximate* time-asymptotic

values when the fresh injection and acceleration are balanced with advection and spreading of high energy particles due to strong diffusion. For strong shocks, $P_{c,2}/\rho_0 V_s^2 \rightarrow 0.56$, where V_s is the shock speed before any significant nonlinear CR feedback occurs. This ratio in the instantaneous shock frame, $P_{c,2}/\rho_0 (V_s')^2$, can as large as 0.9 for $M_s = 133$ shock model, because the shock speed decreases due to nonlinear feedback of CR pressure.

- Once the postshock CR pressure becomes constant, the shock structure evolves approximately in a "self-similar" way, because the scale length of shock broadening increases linearly with time.
- For a given inverse wave-amplitude parameter, ϵ, the CR acceleration efficiency and the flow modification depend sensitively on the shock Mach number, but they seem to converge at the strong shock limit ($M_s \gtrsim 30$).

IV. CR INJECTION AND ACCELERATION EFFICIENCY

We define the injection efficiency as the fraction of particles that have entered the shock from far upstream and then injected into the CR distribution:

$$\xi(t) = \frac{\int_0^{x_{max}} \mathrm{dx} \int_{p_0}^{p_1} 4\pi f_{\mathrm{CR}}(p,x,t) p^2 \mathrm{dp}}{\int n_0 V_s'(t) \mathrm{dt}} \qquad (7)$$

where f_{CR} is the CR distribution function, and n_0 is the particle number density far upstream.

As a measure of acceleration efficiency, we define the "CR energy ratio"; namely the ratio of the total CR energy within the simulation box to the kinetic energy in the *initial shock frame* that has entered the simulation box from far upstream,

$$\Phi(t) = \frac{\int_0^{x_{max}} \mathrm{dx} E_{\mathrm{CR}}(x,t)}{0.5\rho_0 V_s^3 t}. \qquad (8)$$

Since our shock models have the same accretion density and velocity, but different gas pressure depending on M_s, we use the kinetic energy flux rather than the total energy flux to normalize the "CR energy ratio".

In Figure 5 we show the CR energy ratio, Φ, the CR pressure at the shock normalized to the ramp pressure of the upstream flow in the instantaneous shock frame, $P_{c,2}/\rho_0 (V_s')^2$, and the "time-averaged" injection efficiencies, ξ, for shocks with different Mach numbers when $\epsilon = 0.2$ (left three panels). For all Mach numbers the postshock $P_{c,2}$ increases until a balance between injection/acceleration and advection/diffusion of CRs is achieved, and then stays at a steady value afterwards. The time-asymptotic value of the CR pressure becomes, once again, $P_{c,2}/\rho_0 V_s^2 \sim 0.56$ in the initial shock frame, while $P_{c,2}/\rho_0 (V_s')^2 \sim 0.8$ in the instantaneous shock frame for $M_s = 40$ with $\epsilon = 0.2$.

The CR energy ratio, Φ, increases with time as CRs are injected and accelerated, but it asymptotes to a constant value, once $P_{c,2}$ has reached a quasi-steady value. This results from the approximate "self-similar" evolution of the P_c spatial distribution. Time-asymptotic values of Φ increase with M_s and $\Phi \approx 0.5$ for $M_s = 133$ at the terminal time.

In order to explore the dependence of our injection model on the parameter ϵ, especially for low Mach shocks, we also show the results for the $M_s = 3$ models with $\epsilon = 0.2$, 0.25, 0.3, and 0.4 in the right three panels of Figure 5. As expected, the injection rate is higher for larger values of ϵ, so the CR pressure and Φ are higher. In Kang *et al.* (2002), we made a similar comparison for a wider range of Mach numbers and found that the dependence on ϵ is much weaker for stronger shocks.

For strong shocks, the average injection rate is about 10^{-3} with $\epsilon = 0.2$, which corresponds to strong wave generation and inefficient leakage. This injection rate is in fact in a good agreement with what has been observed in the Earth's bow shock (Quest 1988). For $M_s = 3$ shock, the similar injection rate is obtained for $0.25 \leq \epsilon \leq 0.3$, and the CR pressure is about 10-15 % of the shock ram pressure, which could be considered substantial. Then we conclude that CRs can absorb a significant portion of the shock kinetic energy at cosmological shocks, if about $\sim 10^{-3}$ of the particles are injected into the CR component regardless of the details of the injection process.

V. CONCLUSION

There are increasingly more observational evidences that clusters of galaxies and large scale structures may contain a significant amount of cosmic rays and magnetic fields embedded in the tenuous baryonic medium. Several theoretical explanations for origin of those CRs have been proposed, including re-acceleration of relic relativistic electrons by merger shocks, fresh injection/acceleration of CRs at merger shocks, secondary electrons generated by inelastic collisions of CR protons and ICM. Here we have reviewed the scenario in which the diffusive shock acceleration of CR particles at cosmological shocks that formed during the large scale structure formation.

1. We suggest that the CR acceleration at the cosmic shocks are innate to collisionless shock formation process and CRs can absorb a significant fraction of dynamical energy associated with the gravitational collapse during the formation of large scale structure.
2. For strong accretion shocks of $M_s > 10$, CRs can absorb most of shock kinetic energy and the accretion shock speed can be reduced up to 20 %, compared to pure gas dynamic shocks. These shocks typically propagate into the low density intergalactic medium, so the amount of kinetic energy passed through accretion shocks is small.

Since the CR acceleration is the most effective for such strong shocks, the shock flow should be significantly modified by the CR pressure. The accelerated proton spectrum may not be a simple test-particle power-law of p^{-4} because of nonlinear feedback of CR pressure. They might possibly provide acceleration sites for ultra-high energy cosmic rays above 10^{18}eV.

3. For internal merger shocks of $M_s < 3$ the energy transfer to CRs should be less than 10-20 % of the shock kinetic energy at each shock passage, with an associated CR particle fraction of 10^{-3}. These shocks propagate into hot, dense medium in the filaments and the clusters. The spectrum of CR protons should be steeper than $p^{-4.5}$.
4. Cosmic rays and magnetic field could be energetically and dynamically important in the formation of large scale structures. This implies that the current understandings of cosmological hydrodynamic simulations could be modified by inclusion of this process at a quantitative level of order several tens of percent.

This work was supported by grant No. R01-1999-000-00023-0 from the Korea Science & Engineering Foundation.

REFERENCES

Bell, A.R. 1978, The acceleration of cosmic rays in shock fronts. I , MNRAS, 182, 147

Berezhko, E., Ksenofontov, L., & Yelshin, V. 1995, Efficiency of CR acceleration in supernova remnants, Nuclear Physic B., 39, 171.

Berger, J. S., & LeVeque, R. J. 1998, Adaptive Mesh Refinement using Wave-Propagation Algorithms for Hyperbolic Systems, SIAM j. Numer. Anal., 35, 229

Bertschinger, E., 1985, Self-similar secondary infall and accretion in an Einstein-de Sitter universe, ApJS, 58, 39.

Blandford, R. D., & Eichler, D. 1987, Particle Acceleration at Astrophysical Shocks - a Theory of Cosmic-Ray Origin, Phys. Rept., 154, 1

Carilli, C. L., & Taylor, G. B. 2002, Cluster magnetic fields, Annual Rev. Astron. Astrophys., 40, 319

Clark, T.E., Kronberg, P.P., & Böringer, H. 2001, A New Radio-X-Ray Probe of Galaxy Cluster Magnetic Fields, ApJ, 547, L111

Drury, L. O'C. 1983, An Introduction to the Theory of Shock Acceleration of Energetic Particles in Tenuous Plasmas, Rept. Prog. Phys., 46, 9 73

Ensslin, T. A., Lieu, R., & Biermann, P. L., 1999, Nonthermal origin of the EUV and HEX excess emission of the Coma cluster - the nature of the energetic electrons, A&Ap, 344, 409

Feretti, L., Dallacasa, D., Giovannini, G. & Tagliani A., 1995, The magnetic field in the Coma cluster, A&A, 302, 680.

Fusco-Femiano, R., Dal Fiume, D., Feretti, L., Giovannini, G., Grandi, P., Matt, G., Molendi, S., & Santangelo, A. 1999, Hard X-Ray Radiation in the Coma Cluster Spectrum, ApJ, 513, L21

Gieseler U.D.J., Jones T.W., & Kang H. 2000, Time dependent cosmic-ray shock acceleration with self-consistent injection, A&Ap, 364, 911

Giovannini, G., & Feretti, L. 2000. Halo and relic sources in clusters of galaxies, New Astronomy, 5, 335

Jones, T. W., & Kang, H. 1990, Time-dependent evolution of cosmic-ray-mediated shocks in the two-fluid model ApJ, 363, 499

Kang, H., Ryu, D., & Jones, T. W., 1996, Contributions to the Cosmic Ray Flux above the Ankle: Clusters of Galaxies, ApJ, 456, 422

Kang, H., Rachen, J., & Biermann, P. L. 1997, Contributions to the Cosmic Ray Flux above the Ankle: Clusters of Galaxies, MNRAS, 286, 257

Kang, H., Jones, T. W., LeVeque, R. J., & Shyue, K. M. 2001, Time Evolution of Cosmic-Ray Modified Plane Shocks, ApJ, 550, 737

Kang, H., Jones, T. W., & Gieseler, U.D.J, 2002, Numerical Studies of Cosmic-Ray Injection and Acceleration, ApJ, 579, Nov. 1st issue

Kang, H., & Jones, T. W. 2002, Acceleration of Cosmic Rays at Large Scale Cosmic Shocks in the Universe, JKAS, 35, 159

Kang, H., Ryu, D., & Song, D. J., 2002, Large Scale Structure in the universe seen in shocked gas, in preparation

Kim, K.-T., Kronberg, P. P., & Tribble, P. C. 1991, Detection of excess rotation measure due to intracluster magnetic fields in clusters of galaxies, ApJ, 355, 29.

Kronberg, P. P., 1994, Rep. Prog. Phys., 325, 382.

Kulsrud, R. M., Cen, R., Ostriker, J. P., & Ryu, D. 1997, The Protogalactic Origin for Cosmic Magnetic Fields, ApJ, 480, 481

LeVeque, R. J., & Shyue, K. M. 1995, One-dimensional front-tracking based on high resolution wave propagation methods, SIAM J. Scien. Comput. 16, 348

Lieu, R., Ip, W.-H., Axford, W. I., & Bonamente, M. 1999, Nonthermal Origin of the EUV and Soft X-Rays from the Coma Cluster: Cosmic Rays in Equipartition with the Thermal Medium, ApJ, 510, L25

Loeb, A. & Waxmann, E. 2000, Cosmic-ray background from structure formation in the intergalactic medium, Nature, 405, 156

Lucek, S.G., & Bell, A.R. 2000, Non-linear amplification of a magnetic field driven by cosmic ray streaming, MNRAS, 314, 65

Malkov, M.A. 1998, Ion leakage from quasiparallel collisionless shocks: Implications for injection and shock dissipation, Phys. Rev. E, 58, 4911,

Malkov M.A., & Drury, L.O'C. 2001, Nonlinear theory of diffusive acceleration of particles by shock waves, Rep. Progr. Phys. 64, 429

Malkov, M. A. & Völk, H. J., 1998 Diffusive ion acceleration at shocks: the problem of injection, Advances in Space Research, 21, 551

Miniati, F., 2002 Inter-galactic Shock Acceleration and the Cosmic Gamma-ray Background, astro-ph/0203014

Miniati, F., Ryu, D., Kang, H., Jones, T. W., Cen, R., & Ostriker, J. 2000, Properties of Cosmic Shock Waves in Large-Scale Structure Formation, ApJ, 542, 608

Miniati, F., Ryu, D., Kang, H., & Jones, T.W. 2001, Cosmic-Ray Protons Accelerated at Cosmological Shocks and Their Impact on Groups and Clusters of Galaxies, ApJ, 559, 59

Norman C. A., Melrose D. B., & Achterberg A., The Origin of Cosmic Rays above 10 18.5 eV, 1995, ApJ, 454, 60

Quest, K.B. 1988, Theory and simulation of collisionless parallel shocks, J. Geophys. Res. 93, 9649

Ryu, D., Kang, H., & Biermann, P. L. 1998, Cosmic magnetic fields in large scale filaments and sheets, A&AP, 335, 19

Ryu, D., & Kang, H., 1997, Accreting matter around clusters of galaxies: one- dimensional considerations, MNRAS, 284, 416

Ryu, D., Kang, H., Hallman, E., & Jones, T.W., 2002, Cosmological shocks and cosmic rays in the large scale structure of the universe, in preparation

Sarazin, C. L. 1999, The Energy Spectrum of Primary Cosmic-Ray Electrons in Clusters of Galaxies and Inverse Compton Emission, ApJ, 520, 529

Sarazin, C. L., & Lieu, R., 1998, Extreme-Ultraviolet Emission from Clusters of Galaxies: Inverse Compton Radiation from a Relic Population of Cosmic Ray Electrons?, ApJ, 494, L177

Scharf, C. A. & Mukherjee, R., 2002 A statistical detection of gamma-ray emission from galaxy clusters: implications for the gamma-ray background and structure formation, astro-ph/0207411

Sreekumar, P, Bertsch, D. L., Dingus, B. L., Esposito, J. A., Fichtel, C. E., Fierro, J., Hartman, R. C., Hunter, S. D., Kanbach, G., Kniffen, D. A., Lin, Y. C., Mayer-Hasselwander, H. A., Mattox, J. R., Michelson, P. F., von Montigny, C., Mukherjee, R., Nolan, P. L., Schneid, E., Thompson, D. J. & Willis, T. D., 1996, GRET Observations of the North Galactic Pole Region, ApJ, 464, 628

Taylor, G. B., Barton, E. J., & Ge, J. P., 1994, Searching for cluster magnetic fields in the cooling flows of 0745-191, A2029, and A4059, AJ, 107, 1942.

Wentzel, D. G., 1974, Cosmic-ray propagation in the Galaxy - Collective effects, ARAA, 12, 71